Research on Chemical Intermediates (2019) 45:2903–2913
https://doi.org/10.1007/s11164-019-03769-5

Efficient nonthermal plasma degradation of toluene over NiO catalyst with limited NO_x generation

Lu Sun[1] · Wenjun Luo[3] · Wei Sun[1] · Ji Yang[1,2]

Received: 13 November 2018 / Accepted: 5 February 2019 / Published online: 14 February 2019

Abstract

A problem encountered during nonthermal plasma destruction of pollutants in gas streams containing air is that high levels of nitrogen oxides may also be formed as a consequence of the complex processing conditions. In the work presented herein, a post nonthermal plasma catalytic system was evaluated for removal of toluene gas. NiO/γ-Al_2O_3 catalysts with different NiO loadings were prepared via the traditional impregnation method and their activity determined under certain conditions. The effects of the specific input energy (SIE), catalyst calcination temperature, and NiO loading on the toluene degradation were investigated. The catalyst prepared by calcination at 450 °C showed the highest activity. The catalytic activity of the catalysts first increased then decreased with increasing NiO loading, with the maximum toluene conversion of 93 % being achieved by 1.25 wt% NiO/γ-Al_2O_3 at 200 ppm. Meanwhile, the amount of NO_x produced during the reaction was investigated. In the reaction process, a very small amount of NO_x was produced, indicating that the catalyst is green and efficient.

Keywords VOCs · Toluene · Nonthermal plasma · Catalyst

Introduction

Emission of volatile organic compounds (VOCs) from various industrial manufacturing, transport, and indoor sources is an important form of air pollution [1]. As a precursor in the formation of photochemical smog and ground ozone, VOCs

✉ Ji Yang
yangji@ecust.edu.cn

1 School of Resources and Environmental Engineering, State Environmental Protection Key Laboratory of Environmental Risk Assessment and Control on Chemical Process, East China University of Science and Technology, Shanghai 200237, People's Republic of China

2 Shanghai Institute of Pollution Control and Ecological Security, Shanghai 200092, People's Republic of China

3 China Ship Development and Design Center, Shanghai 201108, People's Republic of China

can cause serious injury to public health and the environment, directly or indirectly [2]. Therefore, VOC emissions are subject to stringent environmental regulations and policies in many countries. Conventional methods used to treat VOCs include adsorption [3], absorption [4], condensation [5], membrane separation [6], combustion [7], biological methods [8], and photocatalytic oxidation [9], all of which have shortcomings to some degree. In recent years, nonthermal plasma (NTP) technology has been widely studied for degradation of VOCs because of its simple process and wide application potential [10, 11].

A problem encountered when destroying pollutants in gas streams containing air is that high levels of nitrogen oxides may also be formed as a consequence of the complex processing conditions [12]. Karatum et al. [13] evaluated the efficiency of a dielectric barrier discharge NTP treatment for several common VOCs. When treated as single pollutants at a specific input energy, the removal efficiency was highest for *n*-hexane, reaching 90 %. A promising strategy is to combine NTP and catalysis, which has the potential for enhanced removal with reduced discharge of byproducts. The attractiveness of this hybrid process stems from the possibility to take full advantage of each technology, viz. the high selectivity of catalysis and easy operation of NTP. Compared with commercially available techniques, plasma catalysis for VOC removal can decrease the energy cost while reducing the production of hazardous byproducts.

According to the placement of the catalyst, such coupled plasma–catalysis systems can be divided into two types [14]. Post plasma catalysis (PPC) is a two-stage plasma–catalysis system, including two reactors in series with the catalytic reactor located downstream of the NTP, while in plasma catalysis (IPC) systems, the catalyst is integrated into the reactor. In IPC systems, the plasma contacts the catalyst directly, and reactive species can easily reach the catalyst surface for reaction. In PPC systems, the plasma does not contact with the catalyst directly, and short-lived reactive species produced by the plasma are annihilated before reaching the catalyst bed, thus only species with long lifetime can reach the catalytic reaction zone. In this way, complex homogeneous reactions can occur between the plasma and carrier gas molecules such as O_2, N_2, and VOCs. Due to the low selectivity of NTP, along with oxidation of VOCs to CO_2, this transformation is always accompanied by formation of unwanted hazardous byproducts, e.g., plasma-generated VOCs (reaction intermediates), O_3, and NO_x [15]. In PPC systems, the catalyst downstream from the discharge reactor can effectively decompose the emitted ozone into active oxygen species, improving the oxidation of target VOCs and intermediates as well as suppressing formation of discharge products [16]. The plasma can provide chemically reactive species for further catalysis or preconvert the reactants into more easily converted products to accelerate the catalysis. Therefore, the PPC system can not only enhance the degradation of VOCs, but also decompose byproducts such as O_3, NO_x, and so on. Moreover, the PPC process will not affect the discharge mode or cause discharge instability, and can also reduce coke deposition and avoid catalyst deactivation [17]. The presented work focuses on the application of PPC for toluene removal.

As a representative VOC, toluene was selected as the pollutant in this study. According to previous studies, NiO/γ-Al_2O_3 exhibits excellent catalytic performance

and was thus selected as the catalyst. In this study, the catalysts and plasma were combined in a post nonthermal plasma catalytic (PPC) system by placing the catalyst downstream of the dielectric barrier discharge (DBD) reactor. Although many catalysts are available for plasma catalysis technology, efficient and green ones are lacking.

In this study, the combination of NiO/γ-Al_2O_3 and nonthermal plasma was used for enhanced removal of toluene with reduced NO_x in the waste gas. Meanwhile, factors such as different NiO loadings and calcination temperatures were explored to influence the toluene degradation performance.

Experimental

Experimental setup

The experimental setup consisted of a dielectric barrier discharge (DBD) plasma reactor, catalyst, reaction gas supply system, and analytical instrumentation. The dimensions of the DBD reactor were $500 \times 160 \times 230$ mm^3, with effective discharge length and discharge gap of 25 and 7 mm, respectively.

Experiments were carried out at room temperature and ambient pressure. The temperature change of the catalytic zone was measured by thermocouple. In all of the experiments, the temperature rise in the catalytic zone was negligible. Therefore, any effects observed were the result of nonthermal processes. Toluene was produced by passing purging nitrogen (carrier gas) through pure liquid toluene kept in a water bath ($T = 20 \pm 0.5$ °C); the nitrogen flow rate was adjusted using a mass flow controller. The toluene gas and dilution air were mixed to obtain the desired concentration. For the NTP process, toluene was continuously introduced into the DBD reactor, filling about 0.4 cm^3 of catalyst at the end of the reactor. The catalysts were used under the same conditions, and the reaction conditions were also fixed in similar sets of experiments for better comparison. Alternating-current (AC) power (220 V) at 50 Hz was used to generate nonthermal plasma, with input power of 50 W. The total hydrocarbon content (THC) concentration was analyzed online using a flame ionization detector (FID) detector (Thermo Scientific, Model 51i), which can measure total hydrocarbon emissions from a certain emission source. When the value on the THC analyzer was stable, the plasma reaction was started along with recording of the THC. The decomposition efficiency of toluene in the DBD reactor increased significantly during the first 15 min of discharge, gradually reaching a stable value thereafter. Discharge was continued for at least 40 min until the THC reached a steady state.

The Thermo 51i only detects hydrocarbons in gas phase. Potential byproducts were also determined by gas chromatography (GC)-mass spectrometry (MS). Typically, besides O_3 and NO_x, gas-phase byproducts of toluene degradation mainly include alkanes, aldehydes, acids, benzene series, etc. [18]. In our experiments (Fig. 1), after 40 min of plasma treatment, besides trace amount of toluene, only a negligible amount of acetone was detected in the outlet gas, indicating that the majority of the organic was converted to CO_2. The overall efficiency of toluene

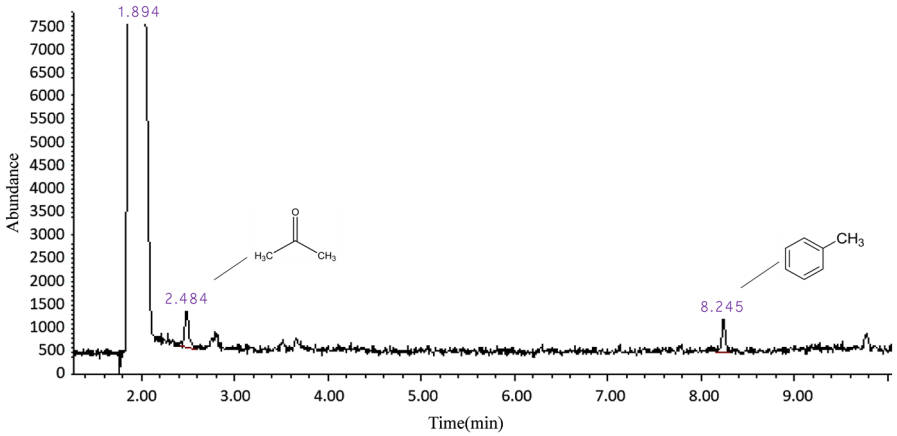

Fig. 1 GC-MS diagram of organic byproducts in the outlet gas

removal (η) can be calculated from the THC. The equation used to calculate the THC conversion was

$$\eta = \frac{C_0 - C_1}{C_0} \times 100\,\%,$$

where C_0 is the initial THC concentration in the system and C_1 is the steady THC concentration after reaction.

Catalyst preparation

A series of NiO/γ-Al_2O_3 catalysts having metal content in the range of 0–16.11 wt% were prepared using impregnation method with commercial γ-Al_2O_3 (40–60 mesh) as support. A certain concentration of $Ni(NO_3)_2$ aqueous solution was impregnated with γ-Al_2O_3 particles. The concentration of the precursor solution was changed according to the target metal loading. After stewing at room temperature for 24 h, it was dried at 120 °C, then calcined in a muffle furnace at 450 °C for 3 h with a heating rate of 5 °C/min. After cooling, it was placed in a dryer for later use. The catalysts with different NiO loadings are denoted as NiO_x/γ-Al_2O_3 ($x = 1.25$, 2.46, 4.10, 6.45, 8.06, 12.31), where x denotes the mass fraction of NiO in each catalyst.

Table 1 ICP-OES results for catalysts

Catalyst	Ni content (wt%)	
	Calculated value (%)	Actual value (%)
$NiO_{1.25}/\gamma\text{-}Al_2O_3$	0.98	0.40
$NiO_{12.31}/\gamma\text{-}Al_2O_3$	9.67	8.7

Table 2 Porous structure parameters of catalysts

Catalyst	A_{BET} ($m^2\ g^{-1}$)	V_{pore} ($cm^3\ g^{-1}$)	D_{pore} (nm)
$\gamma\text{-}Al_2O_3$	235.9	0.48	8.21
$NiO_{1.25}/\gamma\text{-}Al_2O_3$	230.5	0.48	8.30
$NiO_{2.46}/\gamma\text{-}Al_2O_3$	231.5	0.47	8.05
$NiO_{6.45}/\gamma\text{-}Al_2O_3$	216.6	0.45	8.31
$NiO_{8.06}/\gamma\text{-}Al_2O_3$	217.7	0.45	8.19
$NiO_{12.31}/\gamma\text{-}Al_2O_3$	194.0	0.41	8.40

Results and discussion

Catalyst characterization

ICP analysis

Inductively coupled plasma optical emission spectrometry (ICP-OES) was carried out using an Agilent 725ES and used to determine the composition and nickel content of the samples.

As seen from the results in Table 1, the actual loading of NiO was less than the theoretical value. It is presumed that some factors or operations in the process of catalyst preparation or sample pretreatment resulted in the loss of active components.

BET analysis

Nitrogen adsorption apparatus (Micromeritics TriStar 3020 SIN 993) was used to measure the specific surface area and pore characteristics of each catalyst by the multipoint Brunauer–Emmett–Teller (BET) method. The samples were vacuumed for 1 h at 90 °C, then vacuumed for 3 h at 300 °C before analysis.

As seen from the results in Table 2, the specific surface area and pore volume of the catalysts decreased after loading the active component, indicating that the larger pores in the carrier were occupied by active components. The higher BET specific surface area means that the active components were more dispersed, which favors contact between reactants and active components. The pore diameter will affect the residence time of the reaction, and a suitable pore diameter is conducive to reaction of the reactants at the active sites of the catalyst. Smaller pore diameter and larger pore volume mean there is more microreaction space, which is more

conducive to producing reactive species by microdischarge and participation in toluene degradation.

X-ray diffraction analysis

The crystallographic structure of the catalysts was investigated by X-ray diffraction (XRD) analysis. Powder XRD was conducted using a powder diffractometer (*D*/max2550 V apparatus) with Cu K_α radiation ($\lambda = 1.5406$ Å). The data were collected at scattering angles (2θ) ranging from 10° to 80° with step size of 0.02°.

The XRD patterns of the Ni-based catalyst samples are shown in Fig. 2. The typical peaks of NiO appear at 37.248°, 43.275°, and 62.878°. When the NiO loading was low, only the characteristic diffraction peaks of γ-Al_2O_3 appeared, with no diffraction peaks of NiO. Only when the NiO loading was 9.67 % did characteristic diffraction peaks of NiO appear.

X-ray photoelectron spectroscopy

X-ray photoelectron spectroscopy (XPS) was used to determine the surface composition and relative elemental content of the catalysts. The XPS spectra of NiO/γ-Al_2O_3 catalysts with NiO content of 1.25 wt%, 4.10 wt%, and 12.31 wt% are shown in Fig. 3 (Table 3).

It is well known that metal–support interactions will affect the surface properties, thus affecting the catalytic activity of metal catalysts supported on Al_2O_3. The surface distribution of nickel species lying on the surface of the catalysts was investigated in Fig. 3. The split $2p$ electron energy levels Ni $2p_{3/2}$ and Ni $2p_{1/2}$ appeared at 853.9 and 871.5 eV, respectively [19]. The typical oxide structure is also supported

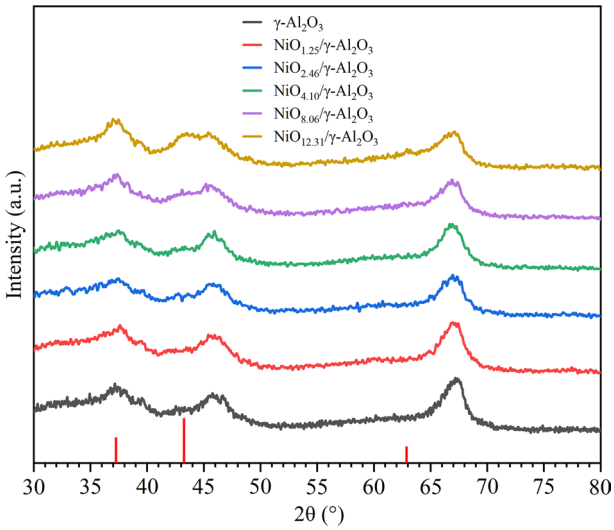

Fig. 2 XRD patterns of the catalysts

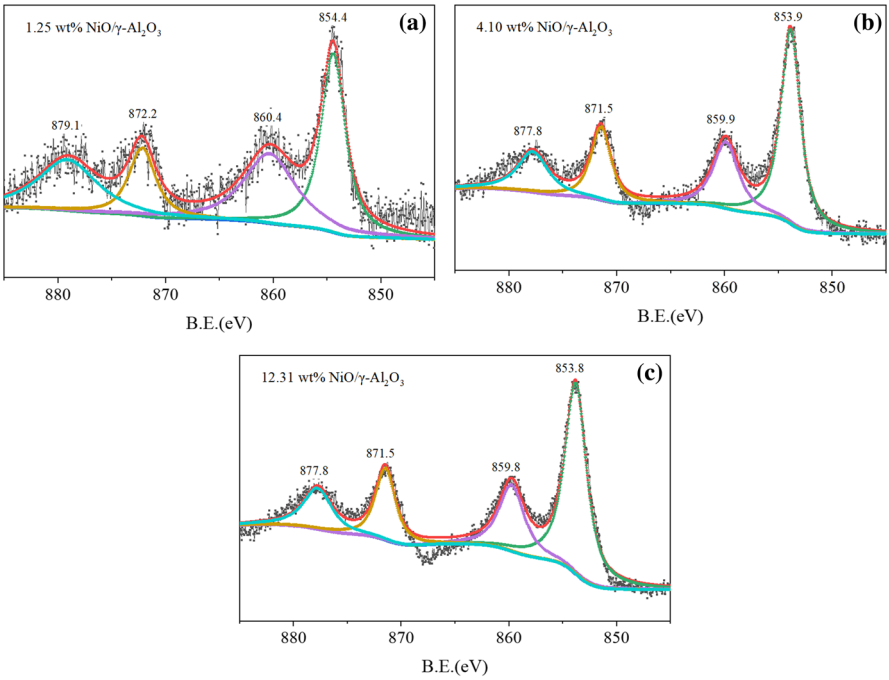

Fig. 3 Ni 2*p* high-resolution XPS spectra of NiO/γ-Al_2O_3 catalysts with different NiO loadings

Table 3 Binding energies (eV) of Ni species of the catalysts

Ni species	NiO loading (wt%)		
	1.25	4.10	12.31
NiO $2p_{3/2}$	854.4	853.9	853.8
NiO $2p_{3/2}$ satellite	860.4	859.9	859.8
NiO $2p_{1/2}$	872.2	871.5	871.5
NiO $2p_{1/2}$ satellite	879.1	877.8	877.8

by the satellite appearing at higher binding energy. The band at about 859.9 eV and 877.8 eV corresponds to the typical shake-up satellite peak, respectively. It is confirmed that the valence of nickel in the catalyst is +2. In a certain range, the interaction between Ni and γ-Al_2O_3 decreases and the peak shifts toward lower binding energy with increasing NiO loading. This also makes it difficult to reduce nickel, degrading the catalytic activity of the catalyst.

Influence of specific input energy

Figure 4 shows the effect of different specific input energy (SIE) conditions on the toluene degradation efficiency. The SIE was changed by altering the airspeed, i.e.,

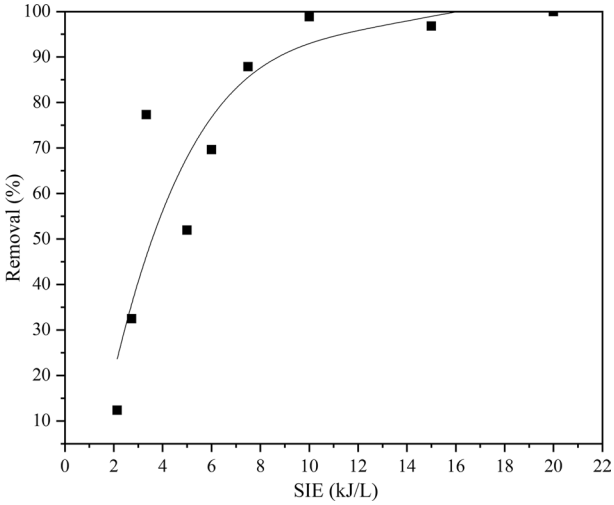

Fig. 4 Effects of SIE on toluene degradation over NTP catalysis system (THC concentration = 200 ppm, flow rate = 0.8 L/min, SIE = 3.75 kJ/L)

the volume of gas flowing through the reactor per hour divided by the discharge area. For constant inlet concentration, the airspeed indicates the residence time of gas in the reactor.

As seen from Fig. 4, the removal of toluene increased with increase of the SIE, but was very low at SIE of 2 kJ/L. When the reactor energy is increased, the number and energy of active particles including electrons, ions, and excited-state particles in the plasma increase, thereby increasing the oxidation reaction and conversion of toluene.

Influence of calcination temperature on catalyst

The calcination conditions have an important influence on the active metal grain size and surface morphology of the catalyst, thus affecting its performance in the reaction. The porous structure parameters of the catalysts were measured by the multipoint BET method. The results are shown in Fig. 5.

The catalysts prepared by calcination at 350 °C and 450 °C showed good catalytic removal performance. The activity of the catalyst obtained by calcination at 450 °C was slightly better than that calcined at 350 °C. However, when the calcination temperature was increased to 550 °C, the catalyst had almost no effect. When the calcination temperature is increased, a large fraction of nickel ions will diffuse into the γ-Al_2O_3. When the calcination temperature is too high, the active species may accumulate on the surface of the catalyst, decreasing the flow of oxygen, weakening the oxidation–reduction ability of the catalyst, and decreasing its activity. The catalyst calcined at 450 °C had more lattice oxygen and more active material, and thus could remove toluene more effectively. The BET results show that the specific surface area of the catalyst calcined at 550 °C was obviously smaller than for the

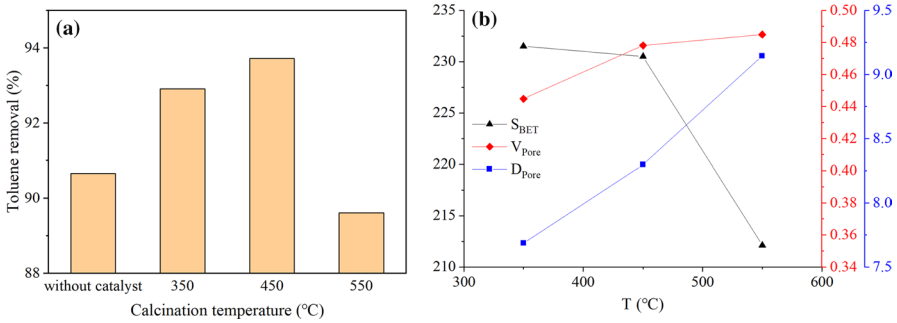

Fig. 5 **a** Effects of calcination temperature on catalytic performance (THC concentration = 200 ppm, flow rate = 0.8 L/min, SIE = 3.75 kJ/L). **b** Porous structure parameters of catalysts with different calcination temperatures

other two catalysts. The specific surface area and pore volume of the catalyst calcined at 450 °C were both large, resulting in the best catalyst.

Influence of NiO loading

The series of NiO/γ-Al_2O_3 catalysts were studied under the same set of reaction conditions, and the changes in the catalytic activity with increasing NiO content investigated. A catalyst containing 0 wt% NiO (only γ-Al_2O_3) was also prepared by modifying the same procedure and used as a reference for all experiments. The effect of the NiO loading on the catalytic activity is shown in Fig. 6, revealing that the content of active components obviously affected the toluene conversion. The catalytic activity of the catalysts first increased then decreased with increasing NiO loading, with the highest toluene removal being achieved for NiO content of 1.25 wt%.

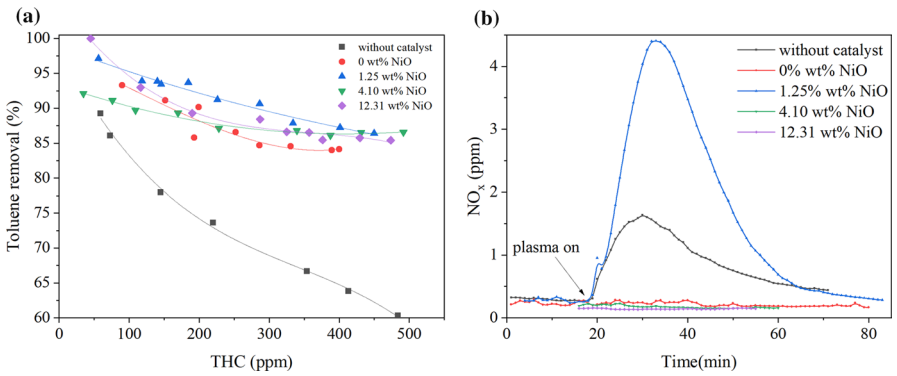

Fig. 6 **a** Effect of NiO loading on toluene degradation over NTP catalysis system. **b** Effect of NiO loading on NO_x generation over NTP catalysis system (THC concentration = 200 ppm, flow rate = 0.8 L/min, SIE = 3.75 kJ/L)

Meanwhile, the NO_x analyzer (Thermo Scientific, Model 42i) was used to determine the amount of NO_x produced during the reaction. The catalysts with different NiO loadings produced a small amount of NO_x in the reaction, with the most being produced in the reaction over $NiO_{1.25}/\gamma\text{-}Al_2O_3$. However, the amount of NO_x produced by all the catalysts was not large, decreasing below 0.5 ppm after the plasma had been on for 40 min. Therefore, it can be said that the $NiO/\gamma\text{-}Al_2O_3$ catalysts produced only a small amount of NO_x in the NTP reaction.

The performance of the catalyst is related to the dispersion state of the active nickel component on the carrier. In the low loading range, nickel is highly dispersed on the surface of $\gamma\text{-}Al_2O_3$. With increased loading, the number of reactive centers exposed to the plasma space increases. When the loading exceeds a certain level, further increase of the loading makes the nickel aggregate into larger particles on the surface area; In other words, increasing the loading will not not increase the number of reactive centers, but will actually lead to a decrease in the number of reactive centers exposed to the plasma space, causing a decrease in the catalytic activity.

The chemical reactions leading to conversion of organic compounds in an air NTP are very complex. Because the plasma reactor and catalyst are separated in a PPC catalytic system, a large number of short-lived active species disappear before reaching the catalyst. The main function of the plasma is to change the composition of the gas entering the catalyst bed and enhance some suitable catalytic reactions. When a PPC system is applied for VOC purification, the role of the plasma is mainly to produce ozone [20]. The bond energy of the C–C bond in the benzene ring is 5–5.3 eV, the bond energy of the C=C bond in the benzene ring is 5.5 eV, and the bond energy of the C–C bond between the methyl and the benzene rings is 4.4 eV, while the energy range of high-energy particles produced by the plasma discharge lies between 1 and 10 eV [21].

When a toluene molecule is attacked by high-energy particles, the mechanism for its decomposition can be divided into three pathways [22]: (1) the methyl group on the benzene ring is dehydrogenated, then benzaldehyde is formed under the action of ·OH, which is further oxidized to benzoic acid; (2) the C–C bond between benzene ring and methyl group breaks, producing benzene, phenol, and other substances under the action of ·OH and ·H; (3) after ring opening, the benzene ring is gradually oxidized to CO_2 and H_2O through a series of reactions.

At present, nonthermal plasma catalytic technology has not yet been widely applied in industry. Future research will mainly focus on reducing the byproducts of the reaction. Due to the variety of industrial waste gases, development of NTP treatment equipment which can treat a variety of pollutants simultaneously will become one of the development directions.

Conclusions

$NiO/\gamma\text{-}Al_2O_3$ catalysts for toluene degradation in a post nonthermal plasma catalytic system were investigated at constant operating conditions (input power 50 W, gas flow rate 0.8 L/min, 100–500 ppm inlet concentration of toluene gas). The degradation of toluene over the $NiO/\gamma\text{-}Al_2O_3$ catalysts decreased with increase of

the airspeed. Experiments were carried out using three catalysts calcined at different temperatures, revealing the best performance at 450 °C. The catalytic performance first improved then reduced with increasing NiO loading of NiO/γ-Al_2O_3. The 1.25 wt% NiO-loaded NiO/γ-Al_2O_3 catalyst showed the best plasma catalytic performance.

Acknowledgements This research is based on work supported by the National Natural Science Foundation of China (51778229).

References

1. W.J. Liang, L. Ma, H. Liu, J. Li, Chemosphere **92**, 10 (2013)
2. K.H. Kim, S.A. Jahan, E. Kabir, Environ. Int. **59**, 41 (2013)
3. X.Y. Zhang, B. Gao, A.E. Creamer, C.C. Cao, Y.C. Li, J. Hazard. Mater. **338**, 102 (2017)
4. K. Bay, H. Wanko, J. Ulrich, Chem. Eng. Res. Des. **84**, A1 (2006)
5. R.J. Davis, R.F. Zeiss, Environ. Prog. Sustain. **21**, 2 (2010)
6. K. Everaert, J. Degreve, J. Baeyens, J. Chem. Technol. Biotechnol. **78**(2–3), 294 (2003)
7. W.B. Li, J.X. Wang, H. Gong, Catal. Today **148**(1–2), 81 (2009)
8. J.M. Estrada, S. Hernandez, R. Munoz, S. Revah, J. Hazard. Mater. **250**, 190 (2013)
9. A.H. Mamaghani, F. Haghighat, C.S. Lee, Appl. Catal. B Environ. **203**, 247 (2017)
10. J.S. Chang, Sci. Technol. Adv. Mater. **2**, 3 (2001)
11. X.X. Feng, H.X. Liu, C. He, Z.X. Shen, T.B. Wang, Catal. Sci. Technol. **8**, 4 (2018)
12. A.M. Harling, J.C. Whitehead, K. Zhang, J. Phys. Chem. A **109**, 49 (2005)
13. O. Karatum, M.A. Deshusses, Chem. Eng. J. **294**, 308 (2016)
14. C.H. Lin, H. Bai, J. Environ. Eng. **127**, 7 (2001)
15. Z. Ye, J.M. Giraudon, N.D. Geyter, R. Morent, J.F. Lamonier, Catalysts **8**, 2 (2018)
16. M.N. Lyulyukin, A.S. Besov, A.V. Vorontsov, Appl. Catal. B Environ. **183**, 18 (2016)
17. H.M. Lee, S.H. Chen, M.B. Chang, S.J. Yu, S.N. Li, Environ. Sci. Technol. **43**, 7 (2009)
18. T. Guo, X. Li, J. Li, Z. Peng, L. Xu, J. Dong, P. Cheng, Z. Zhou, Chemosphere **194**, 139 (2018)
19. M.A. Peck, M.A. Langell, Chem. Mater. **24**(23), 4483 (2012)
20. S. Futamura, A.H. Zhang, H. Einaga, H. Kabashima, Catal. Today **72**(3–4), 259 (2002)
21. Y.F. Guo, D.Q. Ye, K.F. Chen, J.C. He, W.L. Chen, J. Mol. Catal. A Chem. **245**(1–2), 93 (2006)
22. S. Schmid, M.C. Jecklin, R. Zenobi, Chemosphere **79**, 2 (2010)